Vacuum polarization is not a precursor for permanent pair creation

C. Gong[1,2], Q. Su[1] and R. Grobe[1]

(1) Intense Laser Physics Theory Unit and Department of Physics
Illinois State University, Normal, IL 61790-4560, USA

(2) State Key Laboratory for GeoMechanics and Deep Underground Engineering
China University of Mining and Technology, Beijing 100083, China

The effect of an external charge distribution Q on the Dirac vacuum state has been widely studied. For a small magnitude of Q, it can induce a polarization characterized by the displacement of virtual electrons and positrons. If Q is further increased, the occurrence of real and permanent electron-positron pairs is predicted. These well-known findings might suggest that these two phenomena are just the weak- and strong-field limits of the same dynamical vacuum process. However, a direct comparison of these "limits" for a charged capacitor configuration shows that this view is incorrect. The physical mechanisms that lead to the formation of the vacuum's induced polarization charges are entirely different from those that trigger the permanent creation of electron-positron pairs. In fact, computational quantum field theory demonstrates that both phenomena can occur independent of each other; a vacuum decay without any significant polarization is possible and vice versa. This finding allows us also to decompose the total charge density at a given location into the respective contributions from the permanent and the polarization charges.

The quantum electrodynamical interaction of external static as well as electromagnetic fields of various strengths with the vacuum state has received significant attention recently in the intense-laser community [1, 2]. For weaker strengths, the polarization of the vacuum is predicted, as originally discussed by Dirac [3], Heisenberg [4], Serber [5] and Uehling [6] in the mid-thirties. Here short-lived virtual electron-positron pairs are reoriented and can act as temporary electric dipoles. In the presence of an electric field, e.g., the electromagnetic field around a nucleus, these particle–antiparticle pairs reposition themselves, thus partially counteracting and screening the field. The effective field is therefore weaker than would be expected if the vacuum was completely structureless. This leads, for example, to corrections to the well-understood Lamb energy shift or the anomalous magnetic dipole moment of the electron, all of which have been observed experimentally [7].

If the external field (or equivalently the nuclear charge) is increased to become supercritical, it can convert these vacuum bubbles into real physical electron-positron pairs. Historically, this vacuum break-down process has been associated with the pioneering works by Sauter [8] in 1931, Heisenberg and Euler in 1936 [9] and later by Schwinger [10], who gave it a more complete theoretical description in 1951. Here the associated enormous forces inhibit charge re-combinations and separate the electrons and positrons irreversibly. The possibility to experimentally observe this spontaneous breakdown of the vacuum has attracted numerous theoretical studies and also many international laser consortia have invested significant resources into the development of new electromagnetic radiation sources to observe this fascinating relativistic light-matter conversion effect [11,12].

The discussions in the literature as well as similarities between the theoretical descriptions might imply that the two vacuum response mechanisms to external charges with increasing magnitudes are just the weak- and strong-field limit of the same process [13, 14, 15]. This could also suggest that a very strong polarization is actually a required precursor for the consecutive occurrence of the pair creation associated with the permanent vacuum decay process. However, in this communication, we present some data obtained from computational quantum field theory that suggest that these illustrative conceptual ideas can be misleading and that the occurrences of two phenomena are based on entirely different mechanisms.

We report here on two findings deduced from the characteristics of the computed densities for the total charge. First, the vacuum polarization process can occur completely independently of creation of electron-positron pairs associated with the vacuum breakdown. There are certain electric field configurations that produce a significant flux of real pairs while the vacuum polarization is negligible. Alternatively, for other configurations the polarization can be rather large, but not a single permanent electron-positron pair is created.

Second, we suggest that the classical view of comparing the vacuum process to the usual polarization mechanism of a dielectric optical medium [16-18] is inappropriate. In contrast to the polarization of dielectrics, the vacuum's polarization is manifest by the occurrence of charges even in those spatial regions, where the electric field vanishes. The conceptual picture, where a local electric field is solely responsible for inducing the charges in the vacuum, is therefore potentially misleading.

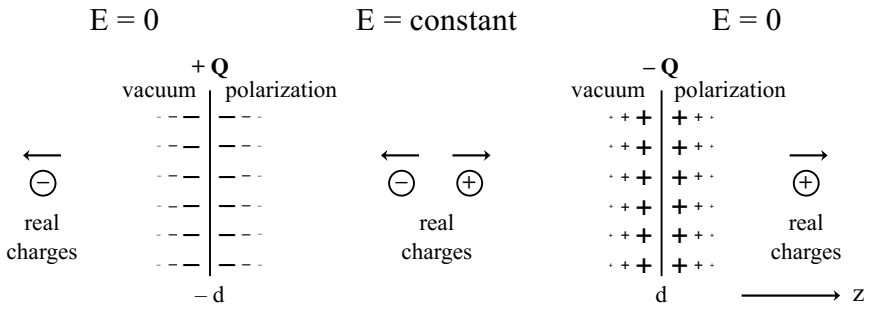

Figure 1 Sketch of the two capacitor plates with the charge densities ±Q and the associated magnitude of the electric field E. We also show the charges associated with the vacuum polarization and those real ones associated with the permanent decay of the vacuum. Note that if there was only a single plate of charge +Q (at z = –d), then its electric field would produce positrons that move to left for z < –d, which is opposite to the current situation where electrons are ejected to the left. The positrons' potential energy decreases linearly from z=–d to d, which accelerates any positive (negative) charge to the right (left). The positive total current density suggests a flow of positive charges to the right and negative charges moving to the left.

To illustrate these points, we have examined in our simulations both the vacuum polarization and the pair-creation for a specific geometry associated with two oppositely charged capacitor plates of separation 2d as sketched in Figure 1. The same configuration of two parallel but uncharged plates was already examined in numerous pioneering studies [19–24] in the context of the Casimir force. In contrast to this work where the fermionic properties of the Dirac vacuum is of interest, there the focus was on the photonic fluctuations associated with the electromagnetic vacuum. A capacitor geometry was also considered recently by Gavrilov and Gitman [25]. Complementary to our studies, which are numerical and focus on the spatial distribution of the charge density due to the vacuum polarization and pair creation, their work employs fully analytically the traditional in- and out- formalism of QED to examine a different aspect. Based on the existence of exact analytical Dirac equation solutions (Weber functions) for the equivalent quantum mechanical particle scattering picture, they compute the vacuum-vacuum transition probabilities and compare their findings to gravitational mechanisms in black holes.

As we will see below, this geometry was chosen as it permits us to study an alternative route to the permanent pair creation than by simply increasing the charges. We assume that the two plates are infinitely

extended in the (x,y) plane and characterized by charge densities ±Q. The resulting electric scalar potential V(z) varies therefore only along the z-direction and can be obtained as a solution from the stationary Maxwell equation $-\partial^2 V(z)/\partial^2 z = 4\pi k_e \rho(z)$, where the associated charge density is given by $\rho(z) = Q\,\delta(z+d) - Q\,\delta(z-d)$ and where Coulomb's constant $k_e \equiv 1/(4\pi\varepsilon_0)$ is related to the vacuum's permittivity ε_0.

The resulting single-step potential takes the form $V(z) = -2\pi k_e Q\,[|z+d| - |z-d|] - 4\pi k_e Q\,d$, characterized by a linear decrease between the plates from $V(z=-d) = 0$ to $V(z=d) = -8\pi k_e Q\,d$. The corresponding electric field follows as $E(z) = -\partial V(z)/\partial z = 2\pi k_e Q\,[(z+d)/|z+d| - (z-d)/|z-d|]$. Its magnitude between the plates ($E = 4\pi k_e Q$) does not depend on the plate spacing 2d. As E is constant between the plates, this region can be considered as a direct local realization of the Schwinger limit [10], which also considers a spatially homogeneous (but infinitely extended) electric field. For our analysis below, it is important to note that E vanishes identically outside the two plates, i.e. for $|z| > d$.

In order to compute the resulting total charge density induced by the two plates, we have employed computational quantum field theory, where the dynamics is modelled by the electron-positron field operator $\Psi(z,t)$. As in this approach the Dirac theory describes solely the fermionic dynamics and the electromagnetic field is considered as an external given force, any photonic fluctuations are neglected throughout this study. Due to the spatial symmetries, we can focus here on only 1+1 space-time dimensions. The operator fulfills simultaneously [26] the time-dependent Dirac equation $i\partial\Psi/\partial t = H\,\Psi$ or, equivalently, the Heisenberg equation of motion $i\,\partial\Psi/\partial t = [h,\Psi]$, where h is the corresponding quantum field theoretical Hamiltonian and the Dirac Hamiltonian is $H = c\,\sigma_1\,p + m\,c^2\,\sigma_3 + e\,V(z,t)$. Here p is the momentum operator and we assume the coupling to a positron with (positive) elementary charge e and mass m. The two 2×2 Pauli-matrices are denoted by σ_1 and σ_3. We focus here on the case where the initial quantum state is void of any matter, i.e., $|\Phi(t=0)\rangle = |\mathrm{vac}\rangle$. We can introduce a set of fermion creation and annihilation operators, denoted by $b(p)^\dagger$, $d(p)^\dagger$, b(p) and d(p), which fulfill the usual fermionic anticommutator relationships, $[b(p),b(p')^\dagger]_+ = \delta(p-p')$ and $[b(p),b(p')]_+ = 0$. When acting on the vacuum state $|\,\mathrm{vac}\rangle$, they excite the modes given by the corresponding single-particle states, i.e., $b_p^\dagger\,|\,\mathrm{vac}\rangle = |\,u;p\rangle$ and $d_p^\dagger\,|\,\mathrm{vac}\rangle = |\,d;p\rangle$ with momentum p, where u and d denotes the states above or below the mass gap between $\pm mc^2$.

Using this (arbitrary) set of basis states for the mode expansion of the field operator $\Psi(z,t)$, we obtain $\Psi(z,t) = \Sigma_p\, b_p(t)\,\phi_p(u;z) + \Sigma_p\, d_p^\dagger(t)\,\phi_p(d;z)$, where $\phi_p(u;z)$ and $\phi_p(d;z)$ are the spatial representations

of the positive and negative energy eigenstates of the field-free Dirac Hamiltonian, given by $H_0 \equiv c\,\sigma_1\,p + \sigma_3\,mc^2$, fulfilling $H_0\,|u;p\rangle = e_p\,|u;p\rangle$ and $H_0\,|d;p\rangle = -\,e_p\,|d;p\rangle$ with $e_p \equiv [m^2c^4+c^2p^2]^{1/2}$. We can express the time-evolved creation and annihilation operators in terms of the initial ones (at t=0) as $b_p(t) = \Sigma_{p'}\,b_{p'}\,\langle u;p\,|u(t);p'\rangle + \Sigma_{p'}\,d_{p'}^{\dagger}\,\langle u;p\,|d(t);p'\rangle$ and $d_p^{\dagger}(t) = \Sigma_{p'}\,b_{p'}\,\langle d;p\,|u(t);p'\rangle + \Sigma_{p'}\,d_{p'}^{\dagger}\,\langle d;p\,|d(t);p'\rangle$. The set of four transition matrix elements $\langle u;p\,|u(t);p'\rangle$, $\langle u;p\,|d(t);p'\rangle$, $\langle d;p\,|u(t);p'\rangle$ and $\langle d;p\,|d(t);p'\rangle$ are the fundamental building blocks of computational quantum field theory (CQFT) [27]. The time-evolution of the creation and annihilation operators is valid for any sub- or supercritical dynamics. Once this set is known, the time-evolution of any desired observable, such as the spatial, momentum or energy densities of the created pair numbers, can be calculated from them. In order to determine all matrix elements, every single state of the Hilbert space $|u;p\rangle$ and $|d;p\rangle$ has to be evolved in time (using $i\partial|\phi\rangle/\partial t = H\,|\phi\rangle$), and then the corresponding projections can be calculated for the corresponding expectation values. The time-dependent Dirac equation was solved on a space-time grid with $N_z \times N_t$ points using a Fourier-transformation based split-operator scheme [28, 29].

The fully-coupled electron-positron field operator $\Psi(z,t)$ itself can be uniquely defined and calculated independently of the basis representation, even for the interesting supercritical field regime, where the number of particles can change in time. As a result, also the total charge density as well as the total electric current density can be obtained unambiguously [30] from the corresponding expectation values of the two operators [31-35], given by $\rho \equiv e\,\Psi^{\dagger}\Psi$ and $J \equiv e\,c\,\Psi^{\dagger}\sigma_1\Psi$,

$$\rho(z,t) \equiv (e/2)\,\Sigma_p\,[\,|\phi_p(d;z,t)|^2 - |\phi_p(u;z,t)|^2\,] \qquad (1.a)$$

$$j(z,t) \equiv (e\,c/2)\,\Sigma_p\,[\,\phi_p(d;z,t)^{\dagger}\,\sigma_1\,\phi_p(d;z,t) - \phi_p(u;z,t)^{\dagger}\,\sigma_1\,\phi_p(u;z,t)\,] \qquad (1.b)$$

which are related to each other via the continuity equation, i.e., $\partial\rho/\partial t + \partial J/\partial z = 0$. Here the summation for $\phi_p(d;z,t)$ and $\phi_p(u;z,t)$ extends over all time-evolved states of the Dirac theory with initial negative and positive energy, respectively. For simplicity, we focus on only one spin direction here. The total charge density $\rho(z,t)$ reflects the contributions due to both the virtual as well as real electron-positron pairs associated with the polarization and vacuum breakdown processes.

For spatially localized electric field configurations such as ours, the threshold condition for the occurrence of real electron-positron pairs is given by the condition that the total potential energy step exceeds twice the mass gap of the Dirac theory, i.e., we require $eV(z = -d) - eV(z = d) \geq 2\,m\,c^2$. This

leads to the threshold requirement $2\,m\,c^2 \leq 8\pi\,k_e\,e\,Q\,d$. This means that there are two independent methods to make our capacitor plate configuration supercritical. We can approach the required field energy between the two plates by increasing either the charge density Q or the plate spacing 2d. This flexibility was the very reason why we examined this particular capacitor configuration in the first place. It allows for a path towards supercriticality while keeping the charge densities Q minimal. As a side note, we remark that both transitions to supercriticality are also accompanied with the diving of the lowest energy from the mass gap into the lower energy continuum.

Let us examine first the vacuum polarization-only regime, i.e., $Q \leq 2m\,c^2/(8\pi\,k_e\,e\,d)$. There are numerous analytical perturbative approaches to determine the resulting polarization charge density. For example, using the perturbative Feynman diagram-based approach, one can compute how the generation of virtual electron-positron pairs gives rise to a modification of the Coulomb potential [36, 37]. Using the one-loop vacuum polarization tensor in 1+1 space-time dimensions, the charge density can be found (up to first order of the fine structure constant α) analytically as $\rho_{pol}(z) = \rho_{single}(z+d) - \rho_{single}(z-d)$. For a single (positively charged) plate we have

$$\rho_{single}(z) = -\,Q\,\alpha\,\hbar\,m^{-1}\,c^{-1}\int_1^\infty d\tau\,\tau^{-3}\,(\tau^2-1)^{-1/2}\exp(-2mc\tau|z|/\hbar) \qquad (2)$$

such that $Q_{pol} = -\,Q\,\alpha\,\hbar\,m^{-2}\,c^{-2}\int_1^\infty d\tau\,\tau^{-4}\,(\tau^2-1)^{-1/2}$ is the total amount of the induced charge, which is the spatial integral over the density $Q_{pol} = \int dz\,\rho(z)$. For a more detailed derivation of this standard approach, one can see Ref. [30]. As a side remark, we note that the integral in Eq. (2) can be approximated such that the single-plate density for $z\neq 0$ is simply given by $\rho_{single}(z) = -\,Q\,(\pi/4)\,\alpha\,\hbar\,m^{-1}\,c^{-1}\exp(-2.35\,m\,c\,|z|\,/\hbar)$.

For the following numerical analysis, we use the convenient atomic units, where c=137.036 and $\hbar = m_e = e = 1$. As the analytical Feynman-based expression Eq. (2) encapsulate the vacuum polarization physics only on the lowest order contributions to $\rho_{pol}(z)$ in Q, it is necessary to establish its validity with regard to our numerical parameter range for Q. In order to do so, we have compared its prediction with three other theoretical approaches, which can compute the polarization density to all orders in Q. All of these three techniques are related to a numerical evaluation of the vacuum expectation value of the charge density operator as provided by the nonperturbative expression (1.a).

The first method evaluates this expression based on the energy eigenvectors of the Dirac Hamiltonian associated given above with the fully dressed vacuum state [38]. For subcritical potentials V(z), these

eigenvectors, defined by H $W_p(d;z,) = w_p(d)\ W_p(d;z,)$ and H $W_p(u;z,) = w_p(u)\ W_p(u;z,)$ with the dressed energies $w_p(d) < -mc^2$ and $w_p(u) \geq -mc^2$, can be obtained by a straightforward diagonalization on a spatial grid. In order to obtain $\rho_{pol}(z)$, $W_p(d;z,)$ and $W_p(u;z,)$ are inserted into the rhs of Eq. (1.a), where they replace the time evolved states $\phi_p(d;z,t)$ and $\phi_p(u;z,t)$.

The second numerical approach for $\rho_{pol}(z)$ is based on the fact that, for the spatial region where the capacitor is located, the bare (force-free) vacuum state evolves in the long-time limit into the dressed vacuum state. This means we can use the time evolved states $\phi_p(d;z,t)$ and $\phi_p(u;z,t)$ in the long-time limit directly in Eq. (1.a). This limit is required to guarantee that some of particles, which were (unavoidably) generated due to the turn-on of the potential V(z), had sufficient time to escape the capacitor. For our geometry, t=0.005 a.u. was fully sufficient to accomplish this. We did not employ any absorption mechanism such as a complex potential at the physical boundaries of our numerical box. The total integration time had to be chosen sufficiently large for the steady state at the plates to be established, but not so long that the created particles can reach the boundaries.

The third approach is computationally the most efficient one as the summation over the infinite many states in Eq. (1.a) can be truncated. The introduction of an energy cut-off for the resulting polarization density, however, requires a subsequent renormalization to recover the correct density. As discussed in more detail Ref. [38,39], this particular procedure can be accomplished by subtracting from the density (with the energy-cut) a different density that is based on the energy eigenvalues of the approximate Foldy-Wouthuysen formulation of the same problem. Here the approximate Hamiltonian given by $H_{FW} \equiv \sigma_3 [m^2c^4 + c^2p^2]^{1/2} + eV(z)$. Due to being diagonal in spinor-space, these states cannot take into account the relativistic couplings between the positive and negative energy states. Therefore, it is ideally suited to subtract out the unphysical contributions to the charge density associated with the energy cut-off [39].

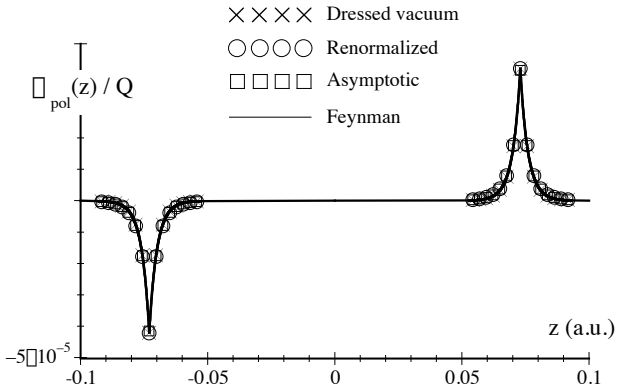

Figure 2 The vacuum polarization charge density induced by the two plates at z = ± d with d=0.073 a.u. and Q = 10 a.u. The four graphs for the charges were computed based on the lowest-order

Feynman perturbative diagram, the eigenvectors associated with the sub-critical dressed vacuum state, the long-time (t = 0.005 a.u.) evolved density according to Eq. (1a) with an energy cut (and the required renormalization) and without an energy cut. The time-evolution of each Hilbert space state was based on $N_t = 5000$ temporal steps using a split-operator scheme and for a numerical box of length L = 2.6 a.u. with $N_z = 8192$ spatial grid points.

In Figure 2 we show the (scaled) vacuum's polarization charge densities $\rho_{pol}(z)/Q$ obtained from all four methods. All four graphs are numerically indistinguishable, giving credence to each approach. The possibility to have several independent computational approaches also helps us to estimate that the magnitude of the (numerically unavoidable) errors is negligible for our parameters. Furthermore, the agreement is perfect for all charge densities Q less than about 100,000 a.u. For larger values, the Feynman based method becomes inapplicable as it is linear in Q and therefore cannot represent the higher order corrections in Q. While the approach based on CQFT and Eq. (1) permits us in principle to observe third (and even higher) order corrections in Q to $\rho(z)$, it shows that the lowest-order Feynman-based approach is remarkably accurate for a wide range of capacitor charge densities Q.

We note that there is a significant charge built up also outside of the capacitor, despite the fact that the electric field vanishes there, as discussed above. This observation is in direct contrast to the predicted polarization density associated with a classical dielectric medium, which is zero in those regions where the electric force field vanishes. This suggests that one has to be careful with comparing the response of the quantum vacuum to an external field with that of a classical dielectric medium.

While we have focused so far on the long-time steady state limit, the computational access to $\rho(z,t)$ permits us also to follow the interesting temporal build-up of the induced polarization as well as permanent real charges. In order to examine the temporal growth of the total charge density for a supercritical field configuration, we have chosen d= 0.073 a.u. and Q = 102443 a.u. such that the resulting potential step far exceeds the threshold for supercriticality as we have here $8\pi\, k_e\, Q\, d = 10\, mc^2$.

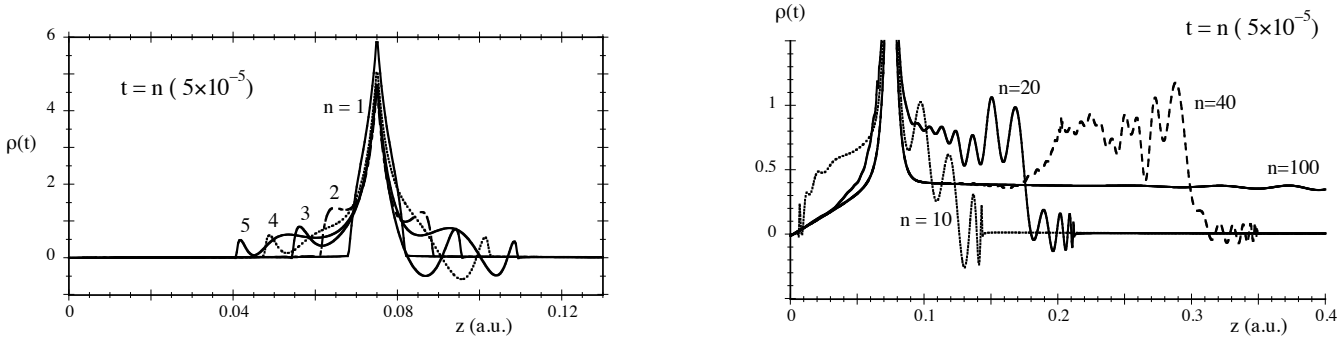

Figure 3 Temporal growth of the total charge density in the supercritical field regime leading in the short-time regime to the steady state density of the vacuum polarization charges and in the long time limit to the steady state of the real pair creation. [Q = 102443 a.u., numerical parameters as in Fig. 2]

In the top of Figure 3, the five temporal snapshots show how the positive vacuum polarization charge grows around the (negatively charged) plate at z = d. While the front portion of the spatially oscillatory density escapes with the speed of light to $z=\pm\infty$, we see a relatively fast occurrence of the steady state of the vacuum polarization charge density. Note that the total area under $\rho_{pol}(z,t)$ close to the plate is not conserved, as the charge conservation law is only a global quantity as $\int_{-\infty}^{\infty} dz\, \rho_{pol}(z,t)$ vanishes only when integrated over the entire domain. As expected, the transient portion of the curve is asymmetric reflecting the different electric fields on each side of the plate. After a short-time scale of the order of c^{-1}, the distribution of the vacuum's virtual charges associated with the polarization approaches its symmetric steady state [given by the long-time limit of Eq. (1.a) and displayed in Fig. 2].

In the bottom graph of Fig. 3, we illustrate the formation of the steady state charge density associated with the vacuum decay process. This process occurs on much longer time scale as the permanently created electron-positron pairs have to travel between both plates before their steady state is created. This steady state is characterized by a spatially constant (positive) density to the right of the right plate ($z>d$), which reflect the constant flow of positrons to $z=\infty$. Similarly (and not shown in the figure), for $z<-d$, we would find a constant flux of permanent electrons that escape to $z=-\infty$. The fact that the density is constant outside the plates (denoted by $\pm\,\rho_{out}$) is expected, as there is no electric force field that could accelerate the generated charges. While this is not so important for our present analysis, we should mention that there are numerous approaches that permit us to calculate (even semi-analytically) the precise value of the outgoing density ρ_{out} as well as the associated particle flux. Most of these techniques rely on Hund's formula [40], which can relate the vacuum's pair creation rate in the steady state to the quantum mechanical transmission coefficient for the associated scattering system [41].

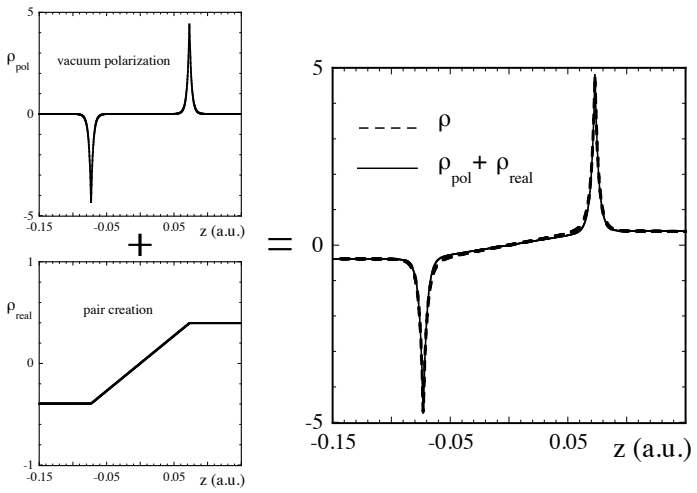

Figure 4 The top left graph shows the charge distribution $\rho_{pol}(z)$ solely associated with the vacuum polarization density around the two plates, (similarly to Fig. 2, but for supercritical field parameter Q=102443 a.u.). The bottom left graph shows the conjectured density $\rho_{real}(z)$ associated solely with the permanent vacuum break down process. In the right Figure we compare the exact total charge density $\rho(z)$ obtained from quantum field theory with the sum $\rho_{pol}(z) + \rho_{real}(z)$.

In Figure 4, we display on a larger spatial scale the resulting steady state distribution $\rho(z)$ of the vacuum polarization as well as the permanent electron-positron pairs. It turns out that this distribution can be reproduced by the *sum* of the vacuum polarization charge ρ_{pol} and the steady state charge ρ_{real} associated with the permanent creation of real electron-positron pairs. The spatial dependence of the vacuum polarization portion $\rho_{pol}(z)$ was already discussed in Figs. 2 and 3. The steady state charge density associated solely with the pair creation process can be approximated by the linear function $\rho_{real}(z) = -\rho_{out}$ for $z \le -d$, $\rho_{real}(z) = \rho_{out}\,[-1+(z+d)/d]$ for $-d \le z \le d$ and finally $\rho_{real}(z) = \rho_{out}$ for $d \le z$.

The agreement between the exact density $\rho(z)$ and $\rho_{pol}(z) + \rho_{real}(z)$ is superb. This is a direct indication that vacuum polarization and real pair creation are two rather independent entities. The appearance of one does not mean at all the disappearance of the other. Alternatively, we could also have established a supercritical plate configuration by keeping the plate separation 2d invariant and increasing Q. However, in this scenario, we do not have a nice spatial separation between the regions of mainly vacuum polarization close to $z = \pm d$, and those between the plates where most of the permanent electron-positron pairs are being created.

In conclusion, we have examined the Dirac vacuum breakdown process triggered by a supercritical field. Contrary to what one might expect, this process is not necessarily the second step following a strong vacuum polarization process. We note that in an interesting recent article by Karbstein [42] the difference between the physical mechanisms for the vacuum polarization and the real pair creation was also

confirmed by their different scaling with the electric field. In fact, in each spatial region it is possible to separate the individual contributions to the total charge density into those that are solely associated with the vacuum polarization mechanism and those contributions associated with permanently created (and moving) charges due to the vacuum breakdown process. The latter finding opens this research field to tackle numerous new fundamental challenges, two of which we outline here briefly.

First, the possible separability to remove ρ_{pol} from ρ in order to study ρ_{real} permits to us to obtain some first insight into the very birth process of particle pairs during the vacuum breakdown process. Here we point out that presently almost all of our knowledge is obtained rather indirectly based on the electron-positron field operator as a mathematical intermediate auxiliary quantity to compute observables such as ρ_{real}. Due to the indirect nature of this theoretical approach, direct equations of motion for ρ_{real} have not been discovered yet, but having now found a method to separate out ρ_{real}, should be a valuable first step towards constructing such a more direct equation for it. This direct equation of motion for $\rho_{real}(z,t)$ would then be a direct analog to the well-known quantum Vlasov equation [43-45], which governs the corresponding momentum density of the created particles for the special case of spatially homogeneous time-dependent fields.

Second, while the charge density ρ_{real} can now be unambiguously accessed inside the supercritical pair creation zone, we still have not developed the corresponding theoretical tools to define an actual particle probability density n(z), except those approximations that are based on projections of the field operators on field-free or incompletely-dressed states [46]. Any proposal to map the supercritical potential V(z) onto n(z), which can be decomposed into its electronic and positronic contributions, $n(z) = n_{e-}(z) + n_{e+}(z)$, could then be tested for consistency with $\rho_{real}(z)$, i.e., we could check the validity of $\rho_{real}(z) = -n_{e-}(z) + n_{e+}(z)$, to gauge the accuracy of such a concept.

Acknowledgements

C.G. would like to thank ILP for the nice hospitality during his visit to Illinois State University and acknowledges the China Scholarship Council program. This work has been supported by the NSF and Research Corporation.

REFERENCES

[1] For a comprehensive review, see, e.g., A. Di Piazza, C. Müller, K.Z. Hatsagortsyan and C.H. Keitel, Rev. Mod. Phys. 84, 1177 (2012).

[2] For a recent review, see, B.S. Xie, Z.L. Li and S. Tang, Matter and Radiation at Extremes 2, 225 (2017).

[3] P.A.M. Dirac, Cambridge Phil. Soc. 30 (2), 150 (1934).

[4] W. Heisenberg, Z. Phys. 90, 209 (1934).

[5] R. Serber, Phys. Rev. 48, 49 (1935).

[6] E.A. Uehling, Phys. Rev. 48, 55 (1935).

[7] A. Antognini, F. Nez, K. Schuhmann, F. D. Amaro, F. Biraben, J. a. M. R. Cardoso, D. S. Covita, A. Dax, S. Dhawan, M. Diepold, et al., Science 339, 417 (2013).

[8] F. Sauter, Z. Phys. 69, 742 (1931).

[9] W. Heisenberg and H. Euler, Z. Phys. 98, 714 (1936).

[10] J.S. Schwinger, Phys. Rev. 82, 664 (1951).

[11] For high power laser systems, see the web sites of the following labs
ELI program: http://www.extreme-light-infrastructure.eu
University of Nebraska-Lincoln: http://www.unl.edu/diocles/index.shtml
European x-ray laser project XFEL: http://xfel.desy.de/
GSI: http://www.gsi.de/fair/experiments/sparc
Vulcan petawatt project: http://www.clf.rl.ac.uk/Facilities/Vulcan/12248.aspx
University of Texas at Austin: http://www.ph.utexas.edu/~utlasers
Stanford: https://slacportal.slac.stanford.edu/sites/lcls_public/
Chinese Academy of Sciences: http://highfield.iphy.ac.cn/
Shanghai Jiaotong University: http://ips.sjtu.edu.cn/

[12] C.N. Danson, C. Haefner, J. Bromage et al, "Petawatt and exawatt lasers worldwide" (Cambridge University Press, 2019).

[13] S. Weinberg, "The quantum theory of fields", Vol. 1, (Cambridge Press, 1995).

[14] M.E. Peskin and D.V. Schroeder, "An introduction to quantum field theory" (Perseus, 1995).

[15] V.B. Berestetskii, E.M. Lifshitz and L. Pitaevskii, "Quantum electrodynamics" (Butterworth-Heinemann, 1980).

[16] R.W. Boyd, “Nonlinear optics” (Academic Press, 2008).

[17] P. Milonni and J.H. Eberly, "Lasers" (Wiley, New York, 1988).

[18] C.C. Gerry and P.L. Knight, “Introductory quantum optics” (Cambridge, 2005).
[19] P.W. Milonni, J.R. Ackerhalt, and W.A. Smith, Phys. Rev. Lett. 31, 958 (1973).
[20] P.W. Milonni and M.-L. Shih, Phys. Rev. A 45, 4241 (1992).
[21] P.W. Milonni, Phys. Rev. A 25, 1315 (1982).
[22] P.W. Milonni, H. Fearn, and A. Zeilinger, Phys. Rev. A 53, 4556 (1996).
[23] R.L. Jaffe, Phys. Rev. D 72, 021301(2005).
[24] J. Schwinger, Lett. Math. Phys. 1, 43 (1975).
[25] S.P. Gavrilov and D.M. Gitman, Phys. Rev. D 93, 045033 (2016).
[26] W. Greiner, B. Müller and J. Rafelski, “Quantum electrodynamics of strong fields” (Springer-Verlag, Berlin, 1985).
[27] T. Cheng, Q. Su and R. Grobe, Cont. Phys. 51, 315 (2010).
[28] A.D. Bandrauk and H. Shen, J. Phys. A 27, 7147 (1994).
[29] J.W. Braun, Q. Su and R. Grobe, Phys. Rev. A 59, 604 (1999).
[30] I. Bialynicki-Birula and Z. Bialynickia-Birula, "Quantum electrodynamics" (Pergamon Press, Oxford, 1975).
[31] E.H. Wichmann and N.M. Kroll, Phys. Rev. 101, 843 (1956).
[32] M. Gyulassy, Phys. Rev. Lett. 53, 921 (1974).
[33] G.A. Rinker and L. Wilets, Phys. Rev. A 12, 748 (1975).
[34] G. Soff and P.J. Mohr, Phys. Rev. A 38, 5066 (1988).
[35] P. Indelicato, P.J. Mohr and J. Sapirstein, Phys. Rev. A 89, 042121 (2014).
[36] For a review, see, e.g., M. D. Schwartz, "Quantum field theory and the standard model" (Cambridge University Press, Cambridge, UK, 2013).
[37] Q.Z. Lv, N.D. Christensen, Q. Su and R. Grobe, Phys. Rev. A 92, 052115 (2015).
[38] Q.Z. Lv, J. Betke, Q. Su and R. Grobe, Phys. Rev. A 92, 032121 (2015).
[39] A.T. Steinacher, J. Betke, S. Ahrens, Q. Su and R. Grobe, Phys. Rev. A 89, 062106 (2014).
[40] F. Hund, Z. Phys. 117, 1 (1941).
[41] Q.Z. Lv, S. Dong, C. Lisowski, R. Pelphrey, Y.T. Li, Q. Su and R. Grobe, Phys. Rev. A 97, 053416 (2018).
[42] F. Karbstein, Phys. Rev. Lett. 122, 211602 (2019).
[43] Y. Kluger, E. Mottola and J.M. Eisenberg, Phys. Rev. D 58, 125015 (1998).
[44] S. Schmidt, D. Blaschke, G. Röpke, S.A. Smolyansky, A.V. Prozorkevich and V.D. Toneev, Int. J. Mod. Phys. E 7, 709 (1998).

[45] F. Hebenstreit, R. Alkofer and H. Gies, Phys. Rev. D 82, 105026 (2010).

[46] C.C. Gerry, Q. Su and R. Grobe, Phys. Rev. A 74, 044103 (2006).